

Magnetic Properties of 2D Nano-Islands Subject to Anisotropy and Transverse Fields: EFT Ising Model

Michel Abou Ghantous¹ & Antoine Khater²

¹ Department of Physics, Science Program, Texas A and M University at Qatar, Education City, Doha, Qatar

² Laboratoire de Physique de l'Etat Condensé UMR 6087, Université du Maine, Le Mans 72085, France

Correspondence: Michel Abou Ghantous, Department of Physics, Science Program, Texas A and M University at Qatar, Education City, PO Box 23874, Doha, Qatar. E-mail: Michel.aboughantous@qatar.tamu.edu

Received: June 23, 2013

Accepted: August 19, 2013

Online Published: August 26, 2013

doi:10.5539/mas.v7n9p63

URL: <http://dx.doi.org/10.5539/mas.v7n9p63>

Abstract

An Ising effective field theory (EFT) is presented to calculate the characteristic magnetic properties of a 2D nano-island presenting an out-of-plane magnetization, and subject to an applied in-plane transverse magnetic field. A non-diagonal Ising Hamiltonian with nearest neighbor exchange, single-atom magnetic anisotropy, and a transverse Zeeman term, defines the ground state of the system. We investigate the effects due to the transverse field acting on the magnetic order, in conjunction with those due to the reduced dimensionalities of the core and periphery domains of the nano-island. The choice of a model spin $S \geq 1$ for the atoms permits the analysis of spin fluctuations via the single-atom spin correlations. A numerical method is developed to avoid approximations inherent to analytical treatments of the non-diagonal Hamiltonian for spin $S \geq 1$ systems. It is applied successfully for nano-island spin $S = 1$ and 2 systems, generating accurate EFT results. Detailed computations are made for the characteristic magnetic properties of the nano-island over its hexagonal lattice, and applied numerically to calculate the properties of the 2D Co nano-island on an fcc(111) surface. It is shown how the transverse magnetic field perturbs the magnetic order, generating spin correlations and magnetizations for the core and periphery domains that are fundamentally different along the longitudinal and transverse directions. The transverse field drives the system Curie temperature to lower values with increasing strength. The isothermal susceptibilities are shown to be exchange dominated along the out-of-plane direction and quasi-paramagnetic in the inplane. A characteristic thermodynamic function that scales directly with the spin and the transverse field is derived for the correlations of the longitudinal and transverse spin components on the nano-island atomic sites.

Keywords: properties of magnetic nano-islands, Ising spin model, nano-islands subject to transverse magnetic fields

1. Introduction

The study of the magnetic properties of nanostructures on surfaces is of current interest because of the potential use of these structures as basic elements in information storage technology. The 2D magnetically ordered nano-islands on metallic and buffer layer substrates, as Co nano islands on Pt, Au, and Ag (Rasponi et al., 2003; Gambardella et al., 2005; Weiss, 2004; Sessi et al., 2010), constitute a promising class. These nano-island systems present out-of-plane magnetic order.

Previously, we gave the Ising spin effective field theory (EFT) for the characteristic magnetic properties of the 2D nano-islands *free* from externally applied magnetic fields (Khater & Abou Ghantous, 2011), and also model calculations for such nano-island systems when subject to magnetic fields applied *out-of-plane* (Abou Ghantous & Khater, 2011).

The purpose of the present paper is to extend the EFT theory to investigate the consequences to the nano-island systems of magnetic fields applied *in-plane*. The present Ising spin model calculations, furthermore, are given for spins $S \geq 1$. These model calculations are applied in particular to compute the characteristic magnetic properties of 2D Co nano-islands on Pt(111) surface.

The influence of an *in-plane* or *transverse* field may be traced back to the work of de Gennes (1963) who introduced this term to take into account the tunneling between two potential wells in ferroelectric crystals. Blinc (1960) introduced the notion of a pseudo-spin 1/2, and Stinchcombe (1973) is the first to use the field theoretical

approach to treat the transverse field in an Ising spin 1/2 model. Kaneyoshi et al. (1993) have considered this transverse field for some cases of higher spin in bulk systems, but neglected the anisotropy.

In more recent years theoretical results have been published which combine the single-atom magnetic anisotropies and transverse magnetic fields (Jiang et al., 1993, 1994; Elkouraychi et al., 1993; Htoutou et al., 2004, 2005; Yüksel, 2010). These are computed using the EFT approach (Kaneyoshi et al., 1979; Sá Barreto et al., 1985; Kaneyoshi et al., 1992; Khater et al., 1992; Fittipaldi, 1992; Tucker, 1994; Kaneyoshi, 2002, 2003). The more recent works consider in particular bulk systems, and honeycomb and square lattice symmetries, with spin $S = 1$. Despite these developments, theoretical results are still lacking for magnetic properties of interest for confined nanostructures, and for spin $S > 1$ systems.

In the present paper we develop a novel approach which avoids analytical approximations inherent to previous theoretical treatments of Ising spin Hamiltonians which present both diagonal and off-diagonal terms (Kaneyoshi et al., 1993; Htoutou et al., 2004, 2005; Yüksel, 2010). This novel approach is general for any spin system. Significantly, our results go to the appropriate limits when we suppress selectively the single-atom magnetic anisotropy or the transverse magnetic field. The model computations are carried out in particular for the hexagonal lattice symmetry, and for the spin $S = 1$ system, as this is the symmetry of Co nano-islands on fcc(111) metallic surfaces, and for the spin $S = 2$ system to illustrate the robustness of the approach. Lower lattice symmetries such as square or honeycomb are treated in a straightforward manner within the present model.

The characteristic magnetic properties are then calculated using the nondiagonal Ising spin Hamiltonian which contains the nearest neighbors exchange, single-atom magnetic anisotropies, and transverse applied magnetic fields. The choice of the spin $S = 1$ for the system corresponds to the Co spin, and permits the analysis of local spin fluctuations via the single site spin correlations, which are responsible for many of the magnetic properties of the nano-island systems (Khater & Abou Ghantous, 2011; Abou Ghantous & Khater, 2011).

Our present computations yield in particular the *longitudinal* and *transverse* components of the single-atom spin correlations, and the domain magnetizations and isothermal susceptibilities, for both the core and periphery domains. The distinction between these domains on the nano-islands is based on their structural differences due to different dimensionalities underlined by an order of magnitude ratio between their corresponding local anisotropies. The magnetic exchange in contrast is the same throughout the system.

The paper is organized as follows. The Ising spin Hamiltonian and required information related to our new EFT theoretical and numerical model approach are presented in section 2. In the following section 3, we apply this model to obtain numerical results for the characteristic magnetic properties for the core and the periphery domains of the nano-island spin $S = 1$ system on a hexagonal lattice, subject to an applied transverse magnetic field. Since higher spin systems can also be treated within the framework of this model, we give elements related to the nano-island spin $S = 2$ system as an example of the new numerical approach validity range. Finally, the conclusions and discussion are presented in section 4.

2. Numerically Generated Ising EFT Model

The general Ising spin Hamiltonian H for a spin S , of an ordered magnetic nano-island system which contains exchange, local magnetic anisotropy, and applied transverse magnetic fields, may be expressed as

$$H = -J \sum_{\langle i,j \rangle} S_{iz} S_{jz} - \sum_i D_i S_{iz}^2 - \Omega \sum_i S_{ix} = \sum_i H_i \quad (1)$$

The local Hamiltonian may then be written as

$$H_i = -x S_{iz} - \Omega S_{ix} - D_i S_{iz}^2 \quad (2)$$

$\langle i, j \rangle$ denotes the sum over all nearest neighbours. J is the magnetic exchange, D_i the single-atom anisotropy, different for core atoms, D_c , and periphery atoms, D_p , and Ω the transverse magnetic field, all in meV energy units. The parametric variables for the core atoms will not carry a subscript in general, whereas those for the periphery atoms shall carry systematically the subscript p . Note that the core and periphery atoms of a nano-island have different coordination numbers $z_c > z_p$, for any considered lattice, and hence different dimensionalities. Note also that the core domain of a nanoisland has a much greater number of atoms than the periphery domain on the nano-island outer boundary; for example, the number of Co periphery atoms does not exceed 15% of the total Co nano-island atoms, as has been experimentally verified (Weiss, 2004).

The exchange energy J induces the spin alignment along the z-direction. In contrast, the off-diagonal applied magnetic Ω field tends to perturb this magnetic order, generating a thermodynamic average for the spin component along the x-direction, and may also induce quantum-mechanical tunneling, flipping spin orientations.

The local Hamiltonian in Equation (3) remains however invariant when S_z goes to $-S_z$ on a site, leaving S_x unchanged under a Z_2 symmetry.

The spin operators of the local Hamiltonians may be correlated in principle for neighboring sites. This problem is considered for the spin $S = 1/2$ system by Sá Barreto et al. (1985) using the EFT approach. However, for higher spin values, as those considered in the present investigation, the approach in the cited reference does not apply. To be able to reach a point where numerical calculations become useful, a decoupling approximation is hence considered in the present work which neglects neighboring site correlations but retains single-site correlations. This maintains the invariance of the thermodynamic magnetic properties under spatial translation for each domain over its dimensionality. It permits the computation of the magnetic properties of the nano-island system for arbitrary temperatures except in the neighborhood of the order-disorder transition temperature T_c when critical fluctuations render inapplicable the EFT approach.

In the mixed Hamiltonian of Equation (1), the single-atom magnetic anisotropy term is diagonal but the transverse magnetic field term is off-diagonal, in the spin states. Kaneyoshi et al. (1993) considered the problem of a bulk system with arbitrary spin subject to a transverse field but neglected the magnetic anisotropy. In recent work (Jiang et al., 1993, 1994; Elkouraychi et al., 1993; Htoutou et al., 2004, 2005; Yüksel, 2010), attempts are made to elaborate analytical approximations towards the diagonalization of the mixed Hamiltonian of Equation (1) for bulk spin $S = 1$ systems. Despite their usefulness these treatments are limited and inapplicable for higher spins.

In contrast in the present model calculations, we fully treat both the diagonal and off-diagonal terms of the mixed Hamiltonian for the nano-island spin $S = 1$ and 2 systems, using a numerically generated EFT method to obtain results directly. This approach avoids the previous analytical approximations, which is a necessary condition because the magnetic properties of the nano-island systems depend in a sensitive manner on the domain and periphery dimensionalities and on their spin correlations (Khater & Abou Ghantous, 2011; Abou Ghantous & Khater, 2011). This numerical approach yields accurate EFT results valid for a wide range of D_i and Ω values.

Using quantum mechanics, the EFT generating functions $f_{Op}(x, D_i, \Omega)$ are evaluated. These are necessary to formulate the thermodynamic averages for the spin operators Op on the domain sites. For example, the matrix representations for S_{iz} and S_{ix} for spin $S = 1$ yield following Equation (2) a local spin Hamiltonian matrix in the form

$$H_i(x, D_i, \Omega) = - \begin{pmatrix} D_i + x & \frac{\Omega}{\sqrt{2}} & 0 \\ \frac{\Omega}{\sqrt{2}} & 0 & \frac{\Omega}{\sqrt{2}} \\ 0 & \frac{\Omega}{\sqrt{2}} & D_i - x \end{pmatrix} \quad (3)$$

The thermodynamic average for a given spin operator Op is calculated as the trace of the product of this operator with the density matrix. Since $H_i(x, D_i, \Omega)$ of Equation (3) is not diagonal, it is necessary to develop an appropriate product. We have consequently developed a symbolic and numerical procedure to treat the matrix function $\text{Exp}[-\beta H_i]$ without analytical approximations. We have extensively checked this symbolic and numerical approach, retrieving exact well known results when the transverse field or the anisotropy are selectively suppressed. This numerical formulation can be applied successfully to higher spin values provided the appropriate decoupling approximations for higher order single site spin operators are adopted.

We present below the general expression, written in the Mathematica code, for the characteristic generating functions f_{Op} , as used in our manipulations of the symbolic and numerical package, where $\beta = 1/kT$ with temperature kT in units of meV

$$f_{Op}(x, D_i, \Omega) = \frac{\text{Tr}[\text{Op.MatrixExp}[-\beta H_i(x, D_i, \Omega)]]}{\text{Tr}[\text{MatrixExp}[-\beta H_i(x, D_i, \Omega)]]} \quad (4)$$

In the limit $\Omega \rightarrow 0$, Equation (4) reduces appropriately to the generating functions derived in previous work for the corresponding systems (Kaneyoshi et al., 1993; Khater & Abou Ghantous, 2011; Abou Ghantous & Khater, 2011). The operation of Exp in Equation (4) is defined in the Mathematica package as the code MatrixExp. To illustrate these generating functions, we give in the appendix the exact Van der Weerden identity for $S = 2$ and its characteristic functions as deduced from Equation (4), omitting the anisotropy therein for simplicity.

The thermodynamic canonical averages in EFT concern the appropriate set of spin operators in the system. For

the present calculation, these are the longitudinal and transverse magnetizations, namely $m_z = \langle S_{zi} \rangle$ and $m_x = \langle S_{xi} \rangle$, the single site component correlations $q_{zz} = \langle S_{zi}^2 \rangle$ and $q_{xx} = \langle S_{xi}^2 \rangle$, and the single site cross correlations $q_{zx} = \langle S_{zi} S_{xi} \rangle = q_{xz} = \langle S_{xi} S_{zi} \rangle$, where i denotes a given site on the core and periphery domains. The computations of these variables are developed using the exact Van der Weerden identities. For spin $S = 1$, for example, this identity is

$$\exp(JS_z \nabla) = S_z^2 \cosh(J\nabla) + S_z \sinh(J\nabla) + 1 - S_z^2 \quad (5)$$

where $\nabla = \partial/\partial x$ is the differential operator. In Equation (5) the operators for the magnetizations S_z and the single site spin correlations S_z^2 are clearly identified under the identity. The EFT approach is general and may be applied to higher spin values with corresponding Van Der Weerden identities, but for these systems one needs to make appropriate decoupling approximations for the multiple-spin correlations as shown for the $S = 2$ system, for example, in the appendix.

The developed Mathematica package that pilots the code to calculate Equation (4) consists of a number of symbolic and numerical procedures. To give an idea of its scale, one manipulates ~ 500 and ~ 1500 terms for the square and hexagonal lattices, respectively. These terms are necessary to compute the canonical averages for each magnetic variable, and their number increases considerably with increasing z_c , reaching ~ 20000 terms for an fcc lattice for $S = 5/2$ systems (Abou Ghantous et al., 2012a, 2012b). The developed package solves these symbolic problems for the needed expressions in a direct way.

For a *core site* pertaining to the nano-island core domain, modeled by a 2D lattice with coordination number z_c , the generating equations that yield the required thermodynamic averages for a given spin operator, $\langle \text{Op} \rangle$, are expressed generically as

$$\langle \text{Op} \rangle = \left\langle \left[\exp(JS_{z_c} \nabla) \right]^{z_c} f_{\text{Op}}(x, D_c, \Omega) \right\rangle_{x=0} \quad (6)$$

A core site interfacing the periphery domain has nearest-neighbor atoms in the core as well as on the periphery domain, which necessitates writing separate generating equations. However, since the core domain is significantly larger than the periphery domain, we neglect the periphery-core exchange interactions for the core Hamiltonian.

All atomic sites pertaining to the periphery domain interface naturally the core domain, and have each r nearest-neighbor atoms on the periphery and s nearest neighbors in the core domain. The required generating equations for a *periphery site* are hence given by

$$\langle \text{Op} \rangle = \left\langle \left[\exp(JS_{z_p} \nabla) \right]^r \left[\exp(JS_{z_c} \nabla) \right]^s f_{\text{Op}}(x, D_p, \Omega) \right\rangle_{x=0} \quad (7)$$

The exponential operators in Equations (6), (7), and (8) are replaced by the Van der Weerden identity of Equation (5) for spin $S = 1$, and should be replaced by the appropriate Van derWeerden identities for any other given spin system. Note that $z_c = 6 > z_p = (r + s)$ for a hexagonal lattice, and that the differential operator has the following property

$$\left\langle e^{a\nabla} \right\rangle f_{\text{Op}}(x, D_i, \Omega) \Big|_{x=0} = f_{\text{Op}}(x + a, D_i, \Omega) \Big|_{x=0} = f_{\text{Op}}(a, D_i, \Omega) \quad (8)$$

Equations (6), (7), and (8) are necessary and sufficient to compute the magnetic properties for the core and periphery domains as detailed as follows.

Equation (6) and Equation (8) for the core domain sites generate in their applications to the site spin operators and single-atom spin correlations, a system of nonlinear polynomial equations in the longitudinal and transverse magnetizations, $m_z(kT; J, D_c, \Omega)$ and $m_x(kT; J, D_c, \Omega)$, and in the single-atom spin correlations $q_{zz}(kT; J, D_c, \Omega)$, $q_{xx}(kT; J, D_c, \Omega)$, and $q_{zx}(kT; J, D_c, \Omega)$. They are self-consistent equations which can be used to solve successively for the magnetic variables of interest. For example, the magnetization m for a *core site* can be calculated from its its characteristic reduced polynomial

$$m_z = \langle S_{z_c} \rangle = a(1)m_z + a(3)m_z^3 + a(5)m_z^5 \quad (9)$$

and the single-atom spin correlations q_{zx} for a *core site* may then be calculated from its characteristic reduced polynomial

$$q_{zx} = \langle S_{z_c} S_{x_c} \rangle = e(0) + e(2)m_z^2 + e(4)m_z^4 + e(6)m_z^6 \quad (10)$$

Equation (7) and Equation (8) for the periphery domain sites generate in their applications, using $r = 2$ and $s = 2$ for the hexagonal lattice, the set of nonlinear polynomials per periphery site for the longitudinal and transverse

magnetizations, $m_{zp}(kT; \Omega, D_p; m_z, q_{zz})$ and $m_{xp}(kT; \Omega, D_p; m_z, m_x, q_{zz})$, and single atom spin correlations $q_{zpp}(kT; \Omega, D_p; m_z, m_x, q_{zz})$, $q_{xpp}(kT; \Omega, D_p; m_z, m_x, q_{zz})$, and $q_{zxp}(kT; \Omega, D_p; m_z, m_x, q_{zz})$. We give here only those for m_{zp} and q_{zxp} as a sample representation

$$m_{zp} = u(0) + u(1)m_{zp} + u(2)m_{zp}^2 + u(4)m_{zp}^4 \quad (11)$$

$$q_{zxp} = p(0) + p(1)m_{zp} + p(2)m_{zp}^2 + p(4)m_{zp}^4 \quad (12)$$

The coefficients $a(n)$, $e(n)$, ..., and $u(n)$, $p(n)$, ..., in Eqs.(9, 10, ..., 11, 12...) are in general extensive polynomial functions of the temperature kT , core variable q_{zz} , and system constants (Ω, J, D_c, D_p). They are determined *exactly* from the numerical results obtained by applying the symbolic and numerical procedures of the Mathematica package code. It is in this sense that Equations (9, 10, ..., 11, 12...) are *accurate numerically generated* results. The ensembles of the nonlinear polynomial equations are obtained directly in our procedure; however, they will not be detailed here because of their extensive symbolic and numerical character.

Higher nano-island spin $S > 1$ systems generate, for the same lattice, higher-order nonlinear polynomial equations, characteristic of the corresponding z_c core, and r and s periphery, coordination numbers.

To obtain unique solutions for the magnetic variables for the core domain, the nonlinear polynomials for m_z and q_{zz} must be satisfied *simultaneously* at all temperatures. Note that Equation (9) admits simple solutions for m_z , which correspond to four for the hexagonal lattice. We have developed a specific procedure to solve for the unique solution of this variable in the entire temperature range, see details in (Khater & Abou Ghantous, 2011; Abou Ghantous & Khater, 2011). Substituting for the physically appropriate root m_z from Equation (9) into the nonlinear polynomial for q_{zz} , we are able to reduce the latter to a polynomial identity in the single-atom spin correlations $q_{zz}(kT; D_c, \Omega)$. The set of the calculated unique physical solutions for m_z and q_{zz} permit in turn the determination of the transverse magnetization $m_x(kT; D_c, \Omega)$, and the single-atom spin correlations $q_{xx}(kT; D_c, \Omega)$ and $q_{zx}(kT; D_c, \Omega)$, for the core domain from Equations (9, 10, ...).

The core domain results are injected in the periphery polynomial equations Equations (11, 12, ...) to obtain the corresponding variables q_{zpp} and m_{zp} for the periphery atoms. These permit in turn the determination of the transverse magnetization m_{xp} , and the correlation variables q_{xpp} and q_{zxp} .

The above results give direct access to the isothermal *longitudinal* and *transverse* susceptibilities, $\chi_z(kT; \Omega)$ and $\chi_x(kT; \Omega)$, for the core and periphery domains, under the influence of the transverse magnetic field. The susceptibilities are calculated in the normalized form

$$X_\alpha \equiv X_\alpha(kT; \Omega) = \left[\langle S_\alpha^2 \rangle - \langle S_\alpha \rangle^2 \right] / kT \quad (13)$$

where $\alpha = x, z$. The longitudinal and transverse susceptibilities, for a *core site*, χ_z and χ_x , and for a *periphery site*, χ_{zp} and χ_{xp} , are consequently calculated using Equation (13).

The characteristic magnetic properties for a nano-island system are consequently computed in a comprehensive manner. The model calculations for the spin $S = 1$ system are applied numerically to compute the magnetic properties for the 2D mono-layer Co nano-islands on nonmagnetic fcc(111) metal surfaces. Since this nano-island system presents a hexagonal lattice symmetry, it is of interest to specifically consider this lattice. The numerical results are computed using the magnetic exchange and core anisotropy constants, $J = 2$ meV and $D_c = -0.1$ meV respectively, characteristic of the 2D Co nano-islands on Pt(111) substrates. The present computations consider in particular the influence of low and high transverse magnetic fields, namely for $\Omega/J = 1/2$ and $\Omega/J = 3$, in comparison with the nearest neighbor magnetic exchange. The EFT model computations for the honeycomb, square and hexagonal lattices show common features for the magnetic properties of the nano-island under an applied transverse field. However, the results presented here are only for the hexagonal lattice.

3. Magnetic Properties of the Hexagonal Nano-Island Under the Influence of a Transverse Magnetic Field

The calculated results for q_{zz} and q_{xx} for the core domain of the Co nanoislands are presented in Figure 1 as a function of temperature, for the considered transverse fields.

The calculated longitudinal and transverse magnetizations, m_z and m_x , for sites in the core domain of the 2D Co nano-island, are presented in Figure 2 as a function of temperature, for the relatively low and high transverse magnetic fields, $\Omega/J = 1/2$ and $\Omega/J = 3$. They are seen to satisfy the required relation $m_z^2 + m_x^2 = S^2 = 1$ at $T = 0K$ for both fields. The order parameter m_z decreases in the ordered phase going to zero at a T_c that corresponds in each case to the selected transverse field. In general m_x increases slightly with temperature in the ordered phase before decreasing monotonically for temperatures $T > T_c$.

Further, it is observed in Figure 2 that T_c decreases with increasing Ω . This is a direct measure of the ability of the applied transverse field term to disrupt and reduce the magnetic order. A potential outcome under a critical transverse field $\Omega \rightarrow \Omega_c$ is to drive the order-disorder transition temperature $T_c \rightarrow 0$, provided the magnitude of the single-atom magnetic anisotropy D_c is sufficient to quench the tri-critical point in the phase diagram (kT_c/J , Ω/J) of the core domain (Miao et al., 2009; Yüksel et al., 2010). The value $D_c = -0.1$ meV for the 2D Co nano-island core domain satisfies these criteria. This potential outcome marks the possibility of a quantum phase transition for the core domain and the nano-island at $T_c \approx 0$, that may be accessed by varying the transverse magnetic field up to Ω_c . Note that the Hamiltonian of Equation (1) is similar to that used for the investigation of quantum critical points (Sachdev, 2001), when Ω is large and the system is near its critical temperature.

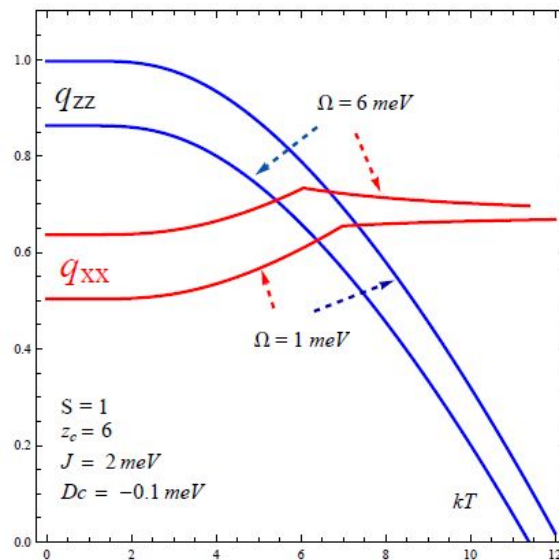


Figure 1. Calculated single-atom spin correlations, q_{zz} and q_{xx} , along the longitudinal and transverse directions, for the core domain of the Co nano-island, as a function of temperature in meV, for relatively low and high transverse fields $\Omega/J = 1/2$ and $\Omega/J = 3$. The hexagonal lattice symmetry and system constants $D_c = -0.1$ and $J = 2$ in meV correspond to Co nano-islands on the Pt(111) surface. The discontinuities of the q_{xx} derivative mark the system T_c for the corresponding Ω values

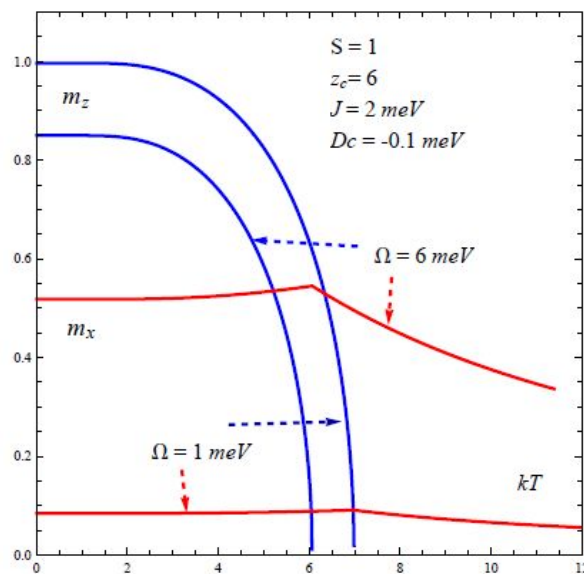


Figure 2. As in Figure 1, for the longitudinal and transverse magnetizations, m_z and m_x , for the core domain of the Co nano-island. The discontinuities of the m_x derivative mark the system T_c for the corresponding Ω values

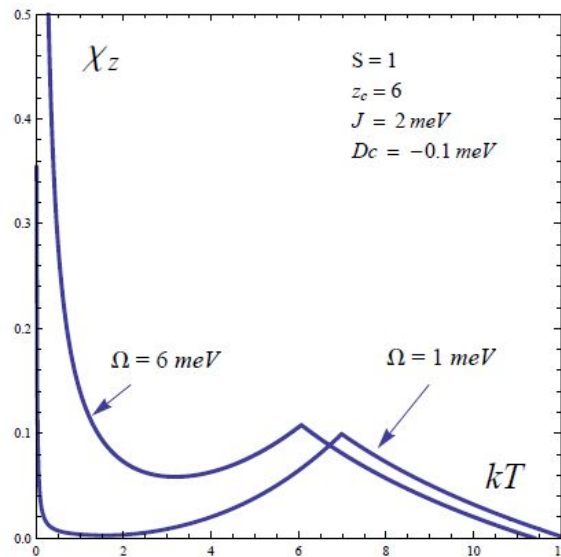


Figure 3. As in Figure 1, for the isothermal longitudinal susceptibility χ_z for the core domain of the Co nano-island. The discontinuities of the χ_z derivative mark the system T_c for the corresponding Ω values

Figure 3 and Figure 4 present our calculated results for the core domain susceptibilities, χ_z and χ_x respectively, as a function of temperature, for the relatively low and high transverse magnetic fields. In Figure 3 the core domain longitudinal susceptibility preserves its character of a second order phase transition, as has been observed for a nano-island spin system free from the applied transverse magnetic field (Khater & Abou Ghantous, 2011; Abou Ghantous & Khater, 2011). An important feature, however, is observed for χ_z at very low temperatures, namely that it starts from large non zero values. The transverse field provokes this, effectively, by reducing q_z and m_z^2 in unequal proportions.

Figure 4(right) gives in particular the calculated results for the inverse susceptibility $1/\chi_x$ of the transverse spin component in the core domain, showing an approximate paramagnetic behavior in the ordered phase for temperatures up to $T \sim T_c/2$. In the region about T_c , it has a complicated behavior due to the decreasing magnetic order. Above T_c the linear slopes of $1/\chi_x$ with temperature point clearly a paramagnetic regime for the transverse spin component in the disordered phase.

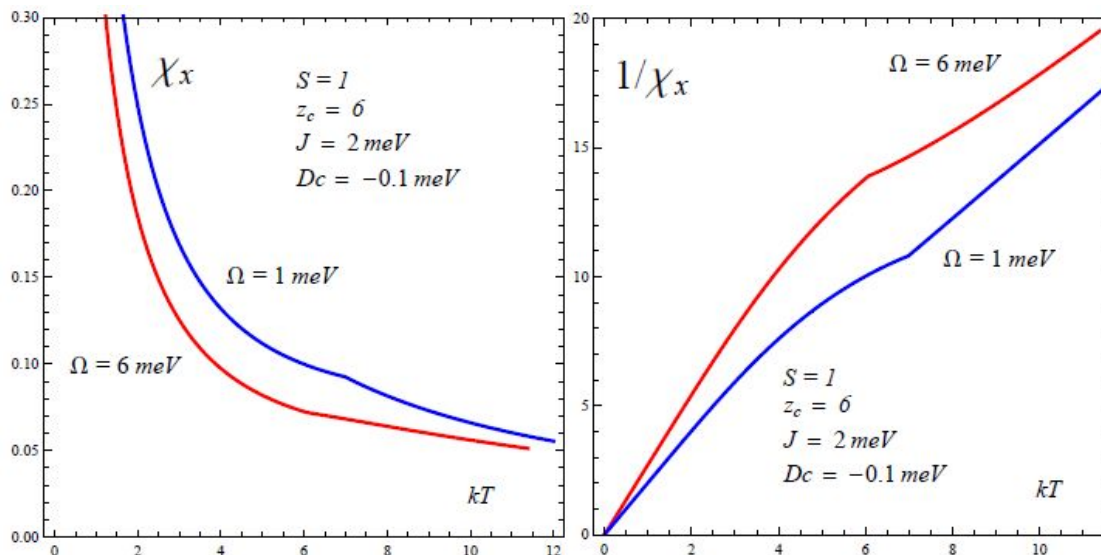


Figure 4. Calculated isothermal transverse susceptibility χ_x (left), and its inverse $1/\chi_x$ (right), for the core domain of the Co nano-island, as in Figure 1. The reciprocal $1/\chi_x$ indicates clearly two limiting paramagnetic regimes for the transverse components of spin in the ordered and disordered phases above T_c .

The model calculations yield equally the correlations for the longitudinal and transverse components of the spin on a single atom, namely $q_{zx}(kT; \Omega) = \langle S_{zc} S_{xc} \rangle$. This prompts us to consider the function $\phi_{zx}(kT; \Omega)$ defined by the following equation

$$q_{zx} = \langle S_x S_z \rangle = \phi_{zx} \langle S_z \rangle \langle S_x \rangle \quad (14)$$

Equation (14) introduces the characteristic thermodynamic function ϕ_{zx} as a measure for the random phase decoupling approximation for the correlations of the longitudinal and transverse spin components on a single atom. We have verified numerically that q_{zx} is symmetric, $q_{zx} = \langle S_z S_x \rangle = \langle S_x S_z \rangle = q_{xz}$, commuting x and z . See also Equation (4). The calculated results for q_{zx} and ϕ_{zx} for the spin $S = 1$ system are presented in Figure 5. Note that ϕ_{zx} is not identical to unity, and that it varies monotonically with temperature in the magnetically ordered phase, $T \leq T_c$. In particular $\phi_{zx}(0; \Omega) = 0.5$ with varying transverse fields.

The numerical calculations are carried out using the same constants for the exchange, the core and the periphery anisotropies, characteristic of the 2D Co nano-islands on Pt(111) substrates. In these calculations we consider again the influence of the relatively low and high transverse fields in comparison with the magnetic exchange, namely $\Omega/J = 1/2$ and $\Omega/J = 3$.

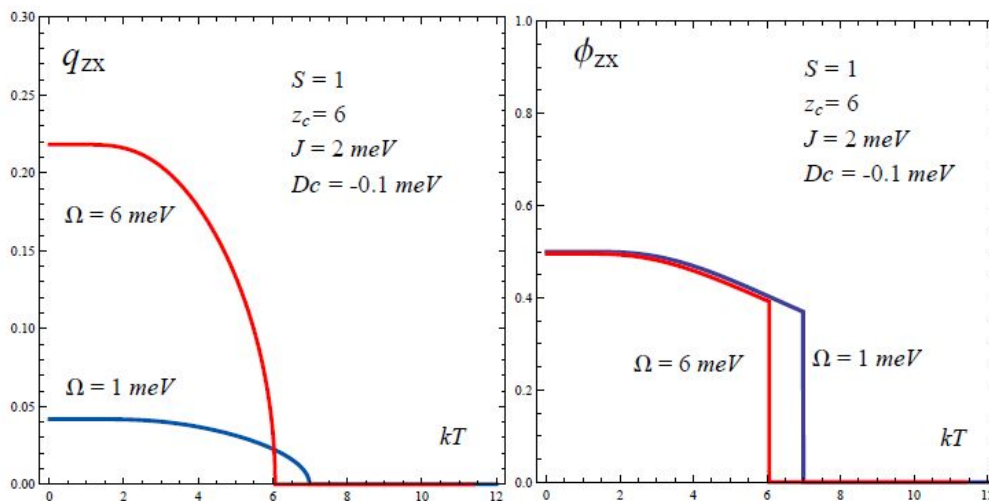


Figure 5. As in Figure 1, (left) single-atom spin correlations, q_{zx} , and (right) characteristic thermodynamic function ϕ_{zx} , for the Co nano-island domain

Figure 6a and Figure 6b present, for respectively low and high transverse fields, the calculated results for the longitudinal and transverse single-atom spin correlations for a periphery site, q_{zxp} and q_{xyp} , in comparison with the longitudinal q_{zz} for a core site. As is physically expected the q_{zxp} decreases whereas the q_{xyp} increases with the transverse field. For a sufficiently high transverse field a crossover temperature exists above which q_{xyp} may become greater than q_{zz} on a periphery site, as in Figure 6b.

The calculated results for the periphery longitudinal and transverse magnetizations, m_{zp} and m_{xp} , are presented in Figure 7, and seen to satisfy the required relation $m_{zp}^2 + m_{xp}^2 = S^2 = 1$ at $T = 0 \text{ K}$ for the considered transverse fields, as is observed for the core magnetizations. However, contrary to the latter, m_{xp} and m_{zp} decrease monotonically at the periphery in the ordered phase going together to zero at T_c . For a given transverse field there is a crossover temperature above which the transverse magnetization becomes greater than the longitudinal magnetization on a periphery site, this is particularly clear for the high transverse magnetic field.

Further, Figure 5a, Figure 5b, and Figure 6 show that the longitudinal and transverse single-atom spin correlations, q_{zxp} and q_{xyp} , and the longitudinal and transverse magnetizations, m_{zp} and m_{xp} , are well defined for the periphery domain in the ordered magnetic phase, $T \leq T_c$, but vanish however in the disordered phase for $T > T_c$. This thermodynamic behavior is a general consequence of the lower dimensionality of the periphery domain in comparison with the core domain, which has been observed previously in the theoretical analysis of the magnetic properties of the 2D Co nano-islands in two other specific cases, namely in the absence of an externally applied magnetic field (Khater & Abou Ghantous, 2011), and under the influence of an applied longitudinal field (Abou Ghantous & Khater, 2011).

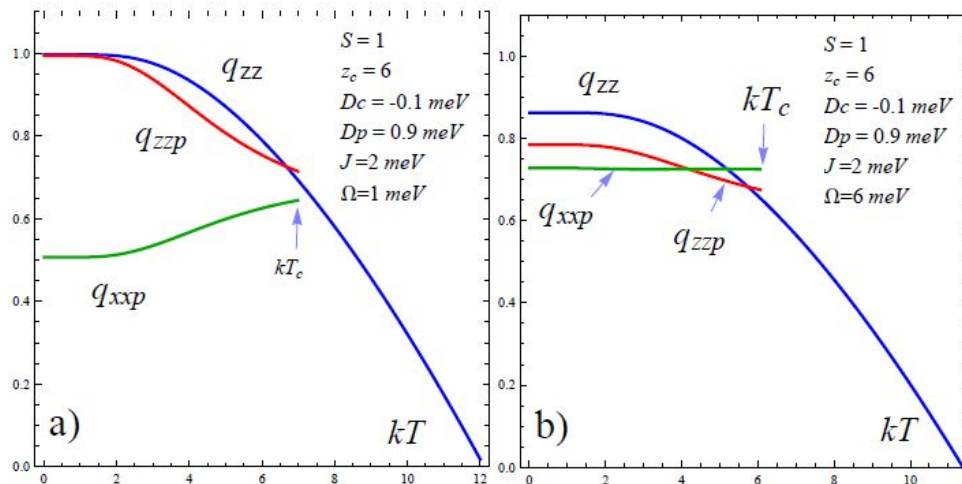


Figure 6. Calculated single-atom spin correlations q_{zxp} and q_{zzp} for the Co nano-island periphery domain, for the relatively low and high transverse fields $\Omega/J = 1/2$ and $\Omega/J = 3$. The q_{zz} for the Co nano-island core domain is indicated for comparison. The hexagonal lattice symmetry and system constants $D_c = -0.1$, $D_p = 0.9$, and $J = 2$ in meV, correspond to Co nano-islands on the Pt(111) surface

The transition temperature T_c is common to the core and periphery nanoisland domains and decreases with increasing transverse field. This implies that under a sufficiently strong critical transverse field $\Omega \rightarrow \Omega_c$, the nanoisland domains approach simultaneously a quantum phase transition at $T = 0$ in the absence of the tri-critical point, as observed previously using the same detailed numerical technique (Khater & Abou Ghantous, 2011).

The isothermal longitudinal susceptibility $\chi_{zp}(kT; \Omega)$ for the periphery domain of the Co nano-island in the presence of the transverse field Ω , is calculated in the normalized form using Equation (13). In Figure 8(left) and Figure 9(left) we present our calculated results for the χ_{zp} for a periphery site as a function of temperature, for respectively low and high transverse fields, in comparison with the χ_z for a core site. Further, it is known that the experimentally measured isothermal longitudinal susceptibility for an ensemble of nano-islands, with statistical variations of the sizes of the core and periphery domains, is effectively a statistical average (Khater & Abou Ghantous, 2011; Abou Ghantous & Khater, 2011). We present hence in Figure 8(right) and Figure 9(right) the calculated total longitudinal susceptibility $\chi_{z;total}$ for an average nano-island configuration putting 15% of its atoms on the periphery, and 85% in the core. Though the core sites present a second order phase transition, it is observed that the nano-island $\chi_{z;total}$ does not strictly present the character of this transition. A discontinuity occurs at $T = T_c$ for low transverse field, while it is absent for relatively high transverse fields.

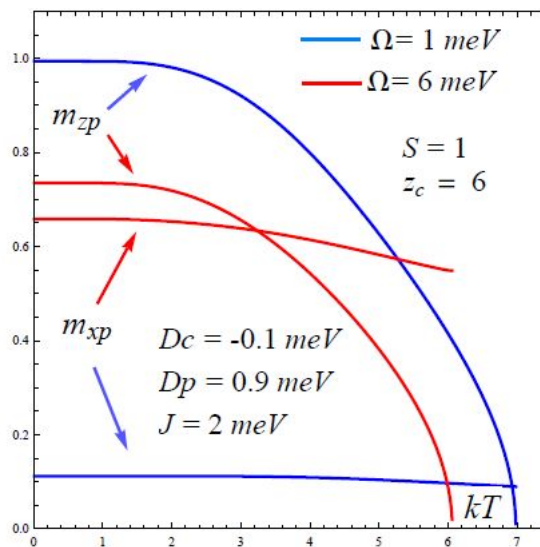


Figure 7. As in Figure 6, for the longitudinal and transverse magnetizations, m_{zp} and m_{xp} , for the Co nano-island periphery domain

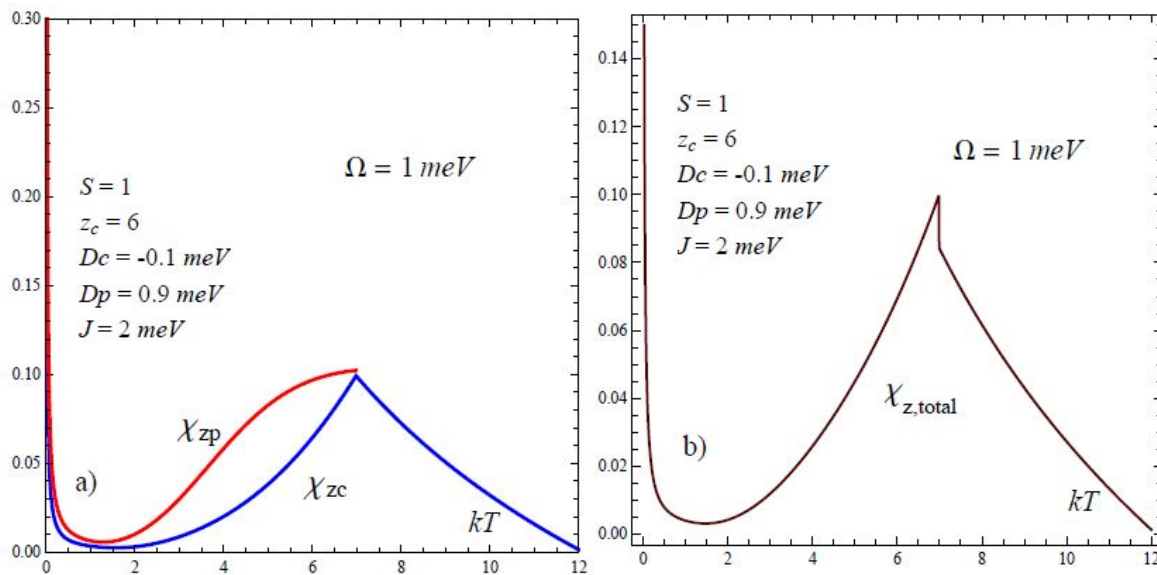


Figure 8. Calculated (left) isothermal longitudinal susceptibility χ_{zp} for the Co nano-island periphery domain as in Figure 6, compared with χ_{zc} for the core domain, for a relatively low transverse field Ω ; (right) longitudinal susceptibility $\chi_{z,total}$ for the Co nano-island, averaged proportionally over the core and periphery domains. See text for details

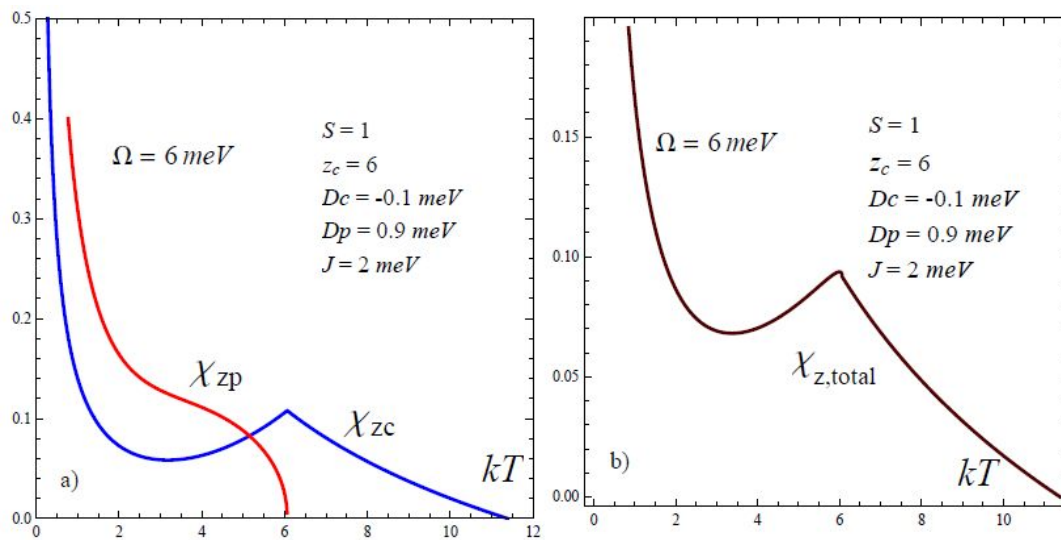


Figure 9. As in Figure 8 for a relatively high transverse magnetic field Ω

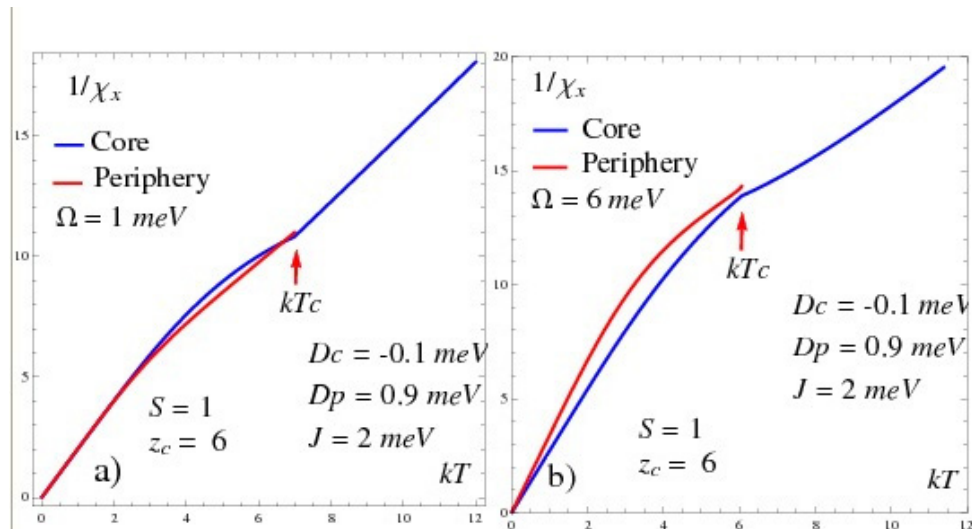


Figure 10. Calculated inverse isothermal transverse susceptibility $1/\chi_{xp}$ for the Co nanoisland periphery domain, for a) relatively low, and b) relatively high transverse fields, in comparison with $1/\chi_x$ at all temperatures for the core domain. Note the crossover of χ_{xp} with respect to χ_x at high transverse fields

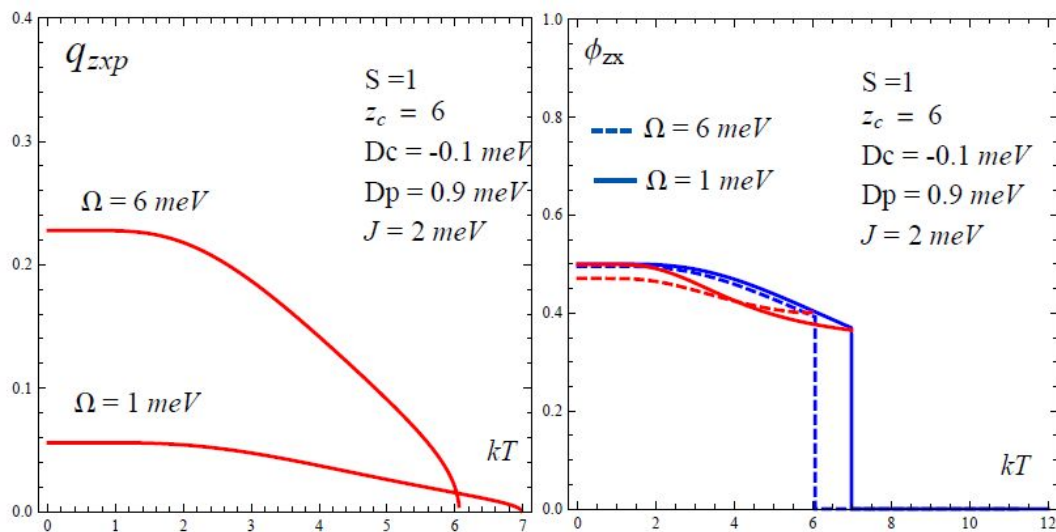


Figure 11. (Left) calculated correlations q_{zxp} , and (right) their characteristic function ϕ_{zxp} for the longitudinal and transverse spin components on a single atom in the Co nanoisland periphery domain. The continuous line and the dashed line in the right figure, correspond to low and high transverse fields respectively. They are shown together with the previous results for the core domain for comparison. See text for details

The inverse isothermal susceptibility $1/\chi_{xp}(kT; \Omega)$ for the transverse spin component in the periphery domain are calculated under the influence of the transverse field, and presented in Fig.10, for respectively the low (left) and high (right) transverse fields. The results show also the crossover of χ_{xp} with respect to χ_x for high transverse fields. These susceptibilities are given in comparison with the inverse isothermal susceptibility $1/\chi_x$ for core sites, and show as for the core domain an approximate paramagnetic behavior in the ordered phase $T \leq T_c$. The linear slopes above the transition temperature, T_c , underline clearly the paramagnetic behavior of the transverse spin component in this domain, in the disordered phase. The model calculations yield equally the correlations for the longitudinal and transverse spin components on an atom in the periphery domain, $q_{zxp}(kT; \Omega) = \langle S_{zp}S_{xp} \rangle$. The calculated results for q_{zxp} for the spin $S = 1$ system are presented in Figure 11(left), for low and high transverse fields. This prompts us further to consider the symmetric function $\phi_{zxp} \equiv \phi_{zxp} = \phi_{zxp}(kT; \Omega)$ for periphery sites defined by an equation equivalent to Equation (11), as in the previous section. In Figure 11(right) we present our calculated results for the function ϕ_{zxp} for two transverse fields values 2 and 6 meV grouping each the periphery sites and core sites curves for comparison. Despite the inflexion in ϕ_{zxp} for periphery sites it is quite comparable

to ϕ_{zx} for core sites, for low and high transverse fields.

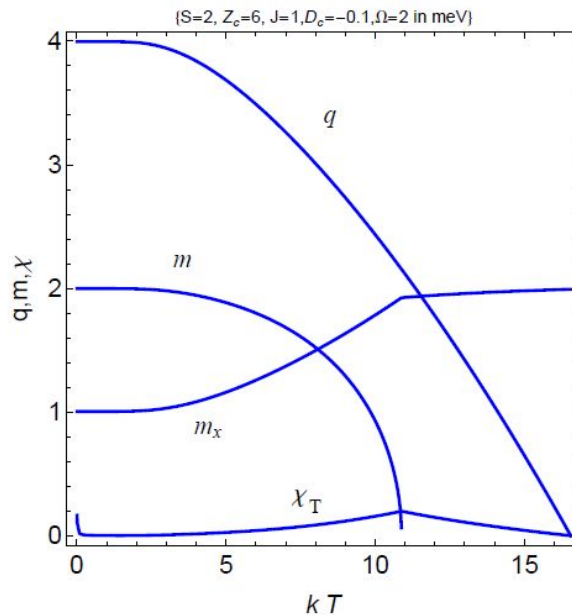


Figure 12. Calculated core magnetic variables m , q , m_x , and χ_T , for the spin $S = 2$ system, showing similarity with the same calculated magnetic variables for the spin $S = 1$ system as presented in previous figures. The system parameters are indicated

Although they are not presented here, we have also calculated the principal magnetic properties for the hexagonal lattice for the spin $S = 2$ nanoisland system, to test the robustness of the method. Comparable forms are derived for the magnetic variables including q_{zx} , ϕ_{zx} , q_{zxp} , and ϕ_{zxp} . In this case however $\phi_{zx}(0; \Omega) = 0.8$. This confirms the observation that the ϕ function presents attributes of a general form scaling directly and simply with the spin and the applied transverse field. In particular, Figure 12 presents the results for the spin $S = 2$. The Van Der Weerden identity and the decoupling approximation are given in the appendix. The same behavior, apart the change of scale with the spin $S = 1$ system, is observed for the q variable. Given the importance of this variable to other quantities, we can use this observation to verify that one can get the result for the spin $S = 2$ system directly from that of the spin $S = 1$ system by scaling the results under the condition that both must have the same critical temperature but with different values of exchange constants J . The verification was better than 10^{-4} . Higher spin systems, for spin $S = 5/2$, and $9/2$, have been investigated in this respect (Abou Ghantous, 2012a, 2012b) related to the island of C_{60}^- adsorbed on buffer surfaces, where the transverse field describes the tunneling between the JT wells in the fullerene anion.

4. Summary and Conclusions

In this work we present an Ising spin EFT model to investigate the consequences of an applied transverse field for the magnetic properties of a 2D mono-layer nano-island. A non-diagonal Ising Hamiltonian with nearest neighbor exchange, single-atom magnetic anisotropy, and a transverse magnetic field term, defines the ground state of the system. The choice of Ising spin $S = 1$ and $S = 2$ systems for the nano-island, permits the analysis of the effects of spin fluctuations via the single-atom spin correlations.

To avoid approximations inherent to previous analytical treatments of the Ising spin Hamiltonian which presents diagonal and off-diagonal terms, a novel symbolic and numerical approach is developed. The procedure consists of using defined codes in Mathematica package for the density matrix over any given characteristic spin operator. It is this numerical property which permits the generation of numerically exact EFT results, valid for a wide range of values for the local anisotropy and applied magnetic transverse fields. This novel approach is general. It can be applied successfully to spin systems higher than $S = 1$, and for diverse 2D lattices such as the honeycomb, square, and hexagonal. Compared to other theoretical and numerical treatments, such as the Monte Carlo simulations, the Ising EFT model remains a robust and useful approach for the study of 2D nano-islands which goes beyond mean field theory.

In particular, we investigate the consequences of an applied transverse magnetic field in conjunction with the

structural effects inherent to the different reduced dimensionalities and their anisotropies on the nano-island core and periphery domains. The principal longitudinal and transverse magnetic properties of the domains of a magnetic nano-island, are computed for relatively low and high transverse fields. Though both the core and periphery domains have a common order-disorder transition temperature, the properties of each are very different, they are also different along the longitudinal and transverse directions. Our model calculations are systematically applied to calculate the characteristic magnetic properties of the magnetically ordered 2D mono-layer Co nano-islands on the Pt(111) surface.

We have primarily developed and presented in this work the model calculations for a hexagonal lattice nano-island, with spin $S = 1$. To test the robustness of our model, we have also applied our method to calculate the magnetic properties of a square lattice nano-island with spin $S = 2$, although these latter results are not presented here.

We show that the temperature behavior of the spin correlations and the magnetizations are fundamentally different for the longitudinal and transverse directions, particularly evident for relatively high transverse fields. This field entails also quite different longitudinal and transverse isothermal susceptibilities for the core and periphery domains, which are seen to be exchange dominated for the out-of-plane, and quasi-paramagnetic for the in-plane, components. Such a configuration yields statistically averaged longitudinal susceptibilities that do not correspond to a second order phase transition for a magnetically ordered nano-island.

Acknowledgments

This research work precedes and is related to work in the NPRP 4-184-1-035 grant from the Qatar foundation.

References

- Abou Ghantous, M., & Khater, A. (2011). Magnetic properties of 2D nanoislands II: Ising spin model. *Journal of Magnetism and Magnetic Materials*, 323, 2504-2512. <http://dx.doi.org/10.1016/j.jmmm.2011.05.027>
- Abou Ghantous, M., Moujaes, E., Dunn, J. L., & Khater, A. (2012a). Cooperative Jahn-Teller effect in a 2D mesoscopic C_{60}^n system with D5d symmetry adsorbed on buffer layers using Ising EFT model. *Eur. Phys. J. B*, 85, 178. <http://dx.doi.org/10.1140/epjb/e2012-30172-5>
- Abou Ghantous, M., Moujaes, E., & Dunn, J. L. (2012b). Ising EFT model applied to 2D mesoscopic C_n-60 islands with a cooperative Jahn-Teller effect. *J. Phys: Conference series, XXI International Symposium on the Jahn-Teller Effect: Physics and Chemistry of Symmetry Breaking*. Tsukuba, Japan.
- Blinic, R. (1960). On the isotopic effects in the ferroelectric behaviour of crystals with short hydrogen bonds. *J. Phys. Chem. Solids*, 13, 204-211. [http://dx.doi.org/10.1016/0022-3697\(60\)90003-2](http://dx.doi.org/10.1016/0022-3697(60)90003-2)
- de Gennes, P. G. (1963). Collective Motions of Hydrogen Bonds. *Solid State Commun.*, 1, 132-137. [http://dx.doi.org/10.1016/0038-1098\(63\)90212-6](http://dx.doi.org/10.1016/0038-1098(63)90212-6)
- Elkouraychi, A., Saber, M., & Tucker, J. W. (1995). On the theory of the transverse Ising model with arbitrary spin. *Physica A*, 213(4), 576-586. [http://dx.doi.org/10.1016/0378-4371\(94\)00240-T](http://dx.doi.org/10.1016/0378-4371(94)00240-T)
- Fittipaldi, I. P., Sarmiento, E. F., & Kaneyoshi, T. (1992). Thermodynamical properties of the spin-one transverse Ising model. *Physica A*, 186(3-4), 591-607. [http://dx.doi.org/10.1016/0378-4371\(92\)90219-G](http://dx.doi.org/10.1016/0378-4371(92)90219-G)
- Gambardella, P., Rusponi, S., Cren, T., Weiss, N., & Brune, H. (2005). Magnetic anisotropy from single atoms to large monodomain islands of Co/Pt(111). *Comptes Rendus Physique*, 6, 75-87. <http://dx.doi.org/10.1016/j.crhy.2004.11.004>
- Honmura, R., & Kaneyoshi, T. (1979). Contribution to the new type of effective-field theory of the Ising model. *J. Phys. C: Solid St. Phys.*, 12, 3979. <http://dx.doi.org/10.1088/0022-3719/12/19/016>
- Htoutou, K., Benaboud, A., Ainane, A., & Saber, M. (2004). The phase diagrams and the order parameters of the transverse spin-1 Ising model with a longitudinal crystal field. *Physica A*, 338, 479-492. <http://dx.doi.org/10.1016/j.physa.2004.01.068>
- Htoutou, K., Oubelkacem, A., Ainane, A., & Saber, M. (2005). Tricritical behaviour in the diluted transverse spin-1 Ising model with a longitudinal crystal field. *Journal of Magnetism and Magnetic Materials*, 288, 259-266. <http://dx.doi.org/10.1016/j.jmmm.2004.09.139>
- Jiang, X. F., Li, J. L., Zhong, J. L., & Yang, C. Zh. (1993). Effect of a crystal field on phase transitions in a spin-1 transverse Ising model. *Phys. Rev. B*, 47, 827-830. <http://dx.doi.org/10.1103/PhysRevB.47.827>
- Jiang, X. F. (1994). Phase transition of the bond-diluted spin-1 transverse Ising model with crystal field

- interaction. *Journal of Magnetism and Magnetic Materials*, 134(1-2), 167-172. [http://dx.doi.org/10.1016/0304-8853\(94\)90088-4](http://dx.doi.org/10.1016/0304-8853(94)90088-4)
- Kaneyoshi, T., Tucker, J. W., & Jaščur, M. (1992). Differential operator technique for higher spin problems. *Physica A*, 186, 495-512. [http://dx.doi.org/10.1016/0378-4371\(92\)90212-9](http://dx.doi.org/10.1016/0378-4371(92)90212-9)
- Kaneyoshi, T., Jaščur, M., & Fittipaldi, I. P. (1993). Transverse Ising model with arbitrary spin. *Phys. Rev. B*, 48, 250-255. <http://dx.doi.org/10.1103/PhysRevB.48.250>
- Kaneyoshi, T. (2000). Decoupling approximation in spin-S ($S/2$) Ising systems. *Physica A*, 286(3-4), 518-530. [http://dx.doi.org/10.1016/S0378-4371\(00\)00356-3](http://dx.doi.org/10.1016/S0378-4371(00)00356-3)
- Kaneyoshi, T. (2003). Phase diagrams of ferroelectric thin films described by the transverse Ising model. *Physica A*, 319, 355-361. [http://dx.doi.org/10.1016/S0378-4371\(02\)01516-9](http://dx.doi.org/10.1016/S0378-4371(02)01516-9)
- Khater, A., Le Gal, G., & Kaneyoshi, T. (1992). Phase diagram of a spin-1/2 bilayer system with disordered interfaces. *Phys. Lett. A*, 171(3-4), 237-241. [http://dx.doi.org/10.1016/0375-9601\(92\)90433-M](http://dx.doi.org/10.1016/0375-9601(92)90433-M)
- Khater, A., Abou Ghantous, M., & Fresneau, M. (2002). A spin-1/2 model for the Curie temperature of binary superlattices containing alloy disordered interfaces. *Journal of Magnetism and Magnetic Materials*, 247(3), 305-315. [http://dx.doi.org/10.1016/S0304-8853\(02\)00283-4](http://dx.doi.org/10.1016/S0304-8853(02)00283-4)
- Khater, A., & Abou Ghantous, M. (2011). Magnetic properties of 2D nanoislands: Ising spin model I. *Journal of Magnetism and Magnetic Materials*, 323, 2717-2726. <http://dx.doi.org/10.1016/j.jmmm.2011.05.011>
- Le Gal, G., Khater, A., & Kaneyoshi, T. (1994). The role of a disordered interface between two ferromagnetic Ising systems in a transverse field. *Physica A*, 209, 129-139. [http://dx.doi.org/10.1016/0378-4371\(94\)90053-1](http://dx.doi.org/10.1016/0378-4371(94)90053-1)
- Miao, H., Wei, G., Liu, J., & Geng, J. (2009). The phase diagrams of a spin-1 transverse Ising model. *Journal of Magnetism and Magnetic Materials*, 321, 102-107. <http://dx.doi.org/10.1016/j.jmmm.2008.08.045>
- Rusponi, S., Cren, T., Weiss, N., Epple, M., Bulushek, P., Claude, L., & Brune, H. (2003). The remarkable difference between surface and step atoms in the magnetic anisotropy of two-dimensional nanostructures. *Nature Materials*, 2, 546-551. <http://dx.doi.org/10.1038/nmat930>
- Sá Barreto, F. C., & Fittipaldi, I. P. (1985). Thermodynamical properties of the transverse Ising model. *Physica A*, 129, 360-373. [http://dx.doi.org/10.1016/0378-4371\(85\)90173-6](http://dx.doi.org/10.1016/0378-4371(85)90173-6)
- Sessi, V., Khunke, K., Zhand, J., Honolka, J., Kern, K., Enders, A., ... Ebert, H. (2010). Cobalt nanoclusters on metal-supported Xe monolayers: Influence of the substrate on cluster formation kinetics and magnetism. *Phys. Rev. B*, 81, 195403. <http://dx.doi.org/10.1103/PhysRevB.81.195403>
- Stinchcombe, R. B. (1973). Thermal and magnetic properties of the transverse Ising model. *J. Phys. C: Solid State Phys.*, 6, 2507. <http://dx.doi.org/10.1088/0022-3719/6/15/011>
- Sachdev, S. (2001). *Quantum Phase Transition*. Cambridge University Press.
- Tucker, J. W. (1994). Generalized Van der Waerden identities. *J. Phys. A: Math. Gen.*, 27, 656-662. <http://dx.doi.org/10.1088/0305-4470/27/3/011>
- Weiss, N. (2004). *Lausanne, Propriétés magnétiques des nano-structures de Co adsorbés*. PhD Thesis. EPFL Lausanne.
- Weiss, N., Cren, T., Epple, M., Rusponi, S., Baudot, G., Rochart, S., ... Brune, H. (2005). Uniform Magnetic Properties for an Ultrahigh-Density Lattice of Noninteracting Co Nanostructures. *Phys. Rev. Lett.*, 95, 157204. <http://dx.doi.org/10.1103/PhysRevLett.95.157204>
- Yüksel, Y., & Polat, H. (2010). An introduced effective-field theory study of spin-1 transverse Ising model with crystal field anisotropy in a longitudinal magnetic field. *Journal of Magnetism and Magnetic Materials*, 322, 3907-3916. <http://dx.doi.org/10.1016/j.jmmm.2010.08.018>

Appendix A. $S = 2$

The Van Der Weerden identity for $S = 2$ is obtained to be

$$\begin{aligned} \exp(JS_{zi}\nabla) &= 1 + \frac{1}{6}S_{zi}(8\sinh(J\nabla) - \sinh(2J\nabla)) + \\ &\frac{1}{12}S_{zi}^2(16\cosh(J\nabla) - \cosh(2J\nabla)) + \\ &\frac{1}{6}S_{zi}^3(-2\sinh(J\nabla) + \sinh(2J\nabla)) + \\ &\frac{1}{12}S_{zi}^4(3 - 4\cosh(J\nabla) + \cosh(2J\nabla)) \end{aligned} \quad (\text{A.1})$$

where β is subsumed in the generating functions f_{op} . used with the decoupling procedure approximation

$$m = \langle S_{zc} \rangle \quad q = \langle S_{zc}^2 \rangle \quad m.q = \langle S_{zc}^3 \rangle \quad q^2 = \langle S_{zc}^4 \rangle \quad m.q^2 = \langle S_{zc}^5 \rangle \quad (\text{A.2})$$

etc. and omitting the anisotropy, the generating functions may be written with $E = (x^2 + \Omega^2)^{1/2}$ in the form

$$f_{sz}(x, 0, \Omega) = \frac{2x(\sinh(\beta E) + 2\sinh(2\beta E))}{E(1 + 2\cosh(\beta E) + 2\cosh(2\beta E))} \quad (\text{A.3})$$

$$f_{sx}(x, 0, \Omega) = \frac{3x^2 + (5x^2 + 2\Omega^2)\cosh(\beta E) + 2(\Omega^2 + 4x^2)\cosh(2\beta E)}{E^2(1 + 2\cosh(\beta E) + 2\cosh(2\beta E))} \quad (\text{A.4})$$

$$f_{s_z^2}(x, 0, \Omega) = \frac{3\Omega^2 + (2x^2 + 5\Omega^2)\cosh(\beta E) + 2(4x^2 + \Omega^2)\cosh(2\beta E)}{E^2(1 + 2\cosh(\beta E) + 2\cosh(2\beta E))} \quad (\text{A.5})$$

However if the anisotropy is present, then Equation (4) must be used.

Copyrights

Copyright for this article is retained by the author(s), with first publication rights granted to the journal.

This is an open-access article distributed under the terms and conditions of the Creative Commons Attribution license (<http://creativecommons.org/licenses/by/3.0/>).